

Intrinsic Fluorescence from DNA Can Be Enhanced by Metallic Particles

Joseph R. Lakowicz, Ben Shen, Zygmunt Gryczynski, Sabato D'Auria,¹ and Ignacy Gryczynski
Center for Fluorescence Spectroscopy, Department of Biochemistry and Molecular Biology, University of Maryland School of Medicine, 725 West Lombard Street, Baltimore, Maryland 21201

Received July 19, 2001

High sensitivity detection of DNA is essential for genomics. The intrinsic fluorescence from DNA is very weak and almost all methods for detecting DNA rely on the use of extrinsic fluorescent probes. We show that the intrinsic emission from DNA can be enhanced many-fold by spatial proximity to silver island films. Silver islands are subwavelength size patches of metallic silver on an inert substrate. Time-resolved measurements show a decreased lifetime for the intrinsic DNA emission near the silver islands. These results of increased intensity and decreased lifetime indicate a metal-induced increase in the radiative rate decay of the DNA bases. The possibility of increased radiative decay rates for DNA bases and other fluorophores suggest a wide variety of DNA measurements and other biomedical assays based on metal-induced increases in the fluorescence quantum yield of weakly fluorescent substances. © 2001 Academic Press

Fluorescence detection is widely used in medical testing and DNA analysis. Extrinsic fluorophores are added covalently and noncovalently to allow DNA detection on gels (1–2), DNA sequencing (3–5), fluorescence *in situ* hybridization (6–7), and for reading of DNA arrays for gene expression (10–11). Extrinsic fluorophores are used because DNA absorbs in the UV near 260 nm. The short absorption wavelength is now less of an obstacle because UV solid state lasers have become available. However, the intrinsic fluorescence from DNA is of little practical usefulness because of the low quantum yields of 10^{-4} to 10^{-5} (12–13).

We now report an approach to obtaining usefully intense intrinsic emission from DNA. This method is general and can be applied to any fluorescent molecule, labeled biomolecule, or in biomedical assays, and is likely to be particularly useful with low quantum yield fluorophores. Our approach relies on a known, but

little used, phenomena of the interactions of excited state fluorophores with metallic surfaces (14–17). Suppose a chromophore is nearly nonfluorescent, as is the case for DNA. The quantum yield (Q) and lifetime (τ) of a fluorophore are given by:

$$Q = \Gamma / (\Gamma + k_{nr}) \quad [1]$$

$$\tau = 1 / (\Gamma + k_{nr}), \quad [2]$$

where Γ is the intrinsic radiative or emissive rate and k_{nr} represents all the other rate processes returning the molecule to the ground state without emission. The low quantum yield of DNA is the result of fast nonradiative decay rates which deplete the excited state prior to significant emission.

One way to increase the quantum yield of a molecule is to increase the radiative rate Γ . However, useful changes in Γ are not possible because this rate is determined by the strengths of the optical transitions, or equivalently the extinction coefficients (18). Alternatively, the quantum yield of some fluorophores can be increased by decreasing the value of k_{nr} , which is typically accomplished by low temperatures or by placement of the fluorophore in a more rigid environment.

It is known that the lifetimes of fluorophores are different when the molecules are within a few wavelengths of a plane silver mirror (19–20). These effects are modest and typically result in no more than 2-fold changes in the lifetime and quantum yield. However, there are more dramatic effects for fluorophores near metallic particles with subwavelength dimensions. Such particles result in amplification of the local electric fields which result in greater excitation of nearby fluorophores. While this effect results in more excitation, the quantum yield is not changed. However, a more important effect is also known to occur.

Metallic ellipsoids with dimensions near 50×100 Å can increase the radiative decay rate of a fluorophore over 1000-fold (14). Suppose a fluorophore has a quantum yield of 0.001, which mean k_{nr} is 1000-fold greater

¹ Permanent address: Institute of Protein Biochemistry & Enzymology, C.N.R., Via Marconi, 10 Napoli, Italy.



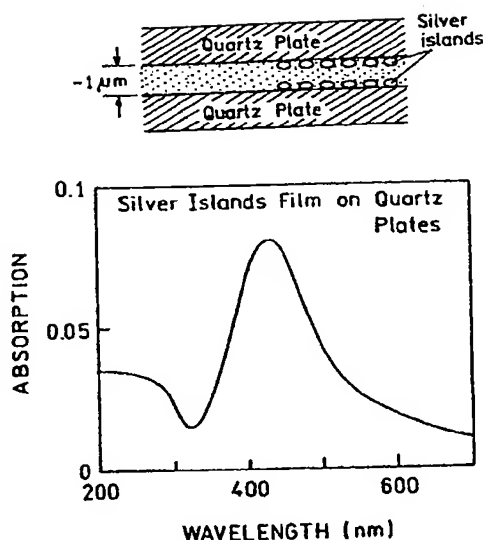


FIG. 1. Top, experimental geometry. Bottom, absorption spectrum of one quartz slide covered with a silver island film.

than Γ (Eq. 1). Now assume the metal particles increase the radiative rate Γ by 1000-fold. In this case the quantum yield will be increased from 10^{-3} to near 0.5. In fact, when using metallic particles to enhance fluorescence it can be advantageous to use low quantum yield fluorophores. Then only those fluorophores at the appropriate distance from the metal surface will fluoresce. In fact the lowest quantum yields may be preferable because the maximum increase in the quantum yield near a metal particle due to an increased radiative rate is $1/Q$ (17).

MATERIALS AND METHODS

Silver particles were prepared using silver nitrate (99+%), sodium hydroxide (pellets, 97%), ammonium hydroxide (NH_3 content 28–30%), and D-glucose (99.5%) all purchased from Aldrich and used without further purification. Silver island films were prepared on quartz plates as described by (21). The quartz slides were soaked in a 10:1 (v/v) mixture of H_2SO_4 (95–98%) and H_2O_2 (30%) overnight before deposition. They were washed with Millipore water and air-dried prior to use. Silver deposition was carried out in a clean 30-ml small beaker equipped with a Teflon-coated stir bar. To a rapidly stirred silver nitrate solution (0.22 g in 26 ml of Millipore water), eight drops of fresh 5% NaOH solution was added. Dark-brownish precipitates were formed immediately. Less than 1 ml of ammonium hydroxide was soon added drop by drop to redissolve the precipitates. Then, the clear solution was cooled down to 5°C in an ice bath, followed by soaking the cleaned and dried quartz slides in the solution. At 5°C , a fresh solution of glucose (0.35 g in 4 ml of water) was added. The mixture was stirred for 2 min at that temperature. Subsequently, the beaker was removed from the ice bath and allowed to warm up to 30°C . As the color of the slides become greenish, the slides were removed and washed with Millipore water and sonicated in a bath sonication for 1 min at room temperature. After rinsing several times with water, the slides were stored in water for several hours prior to the experiments. Calf-thymus DNA was obtained from Sigma and dissolved in 50 mM Tris, pH 7. The DNA concentration was 5 mM as base pairs. Emission spectra were measured on a SLM

8000 spectrofluorometer with 287 nm excitation. Frequency-domain lifetime measurements were obtained on a 10 GHz instrument (22). The excitation source was a cavity-dumped rhodamine 6G dye laser providing approximately 100 ps pulses which were frequency-doubled at 287 nm. Intensity decays were measured through a combination 344 nm interference filter plus a WG 335 long pass filter, which provided transmission from about 330 to 355 nm. Emission spectra and lifetimes were measured with vertically polarized excitation and horizontally polarized emission. This optical configuration reduced scattered light of the excitation wavelength without significant distortion of the spectra or lifetimes. The frequency-domain data were fit to the multi-exponential model where the intensity decay is given by

$$I(t) = \sum_i \alpha_i \exp(-t/\tau_i), \quad [3]$$

where α_i are amplitude factors associated with each decay time τ_i . The sum of the α_i values are normalized to unity, $\sum \alpha_i = 1.0$.

RESULTS

We obtained suitable silver particles by chemical reduction of silver onto quartz microscopic slides (21). The mass thickness is restricted to near 40 Å one obtain particles on the surface with subwavelength dimensions, as can be seen from the characteristic surface plasmon absorption spectrum which are close to the small wavelength limit (Fig. 1). The DNA samples were placed between two such silver islands plates with a separation near 1–1.5 μm . The absorption spectrum for DNA between the plates is approximately the

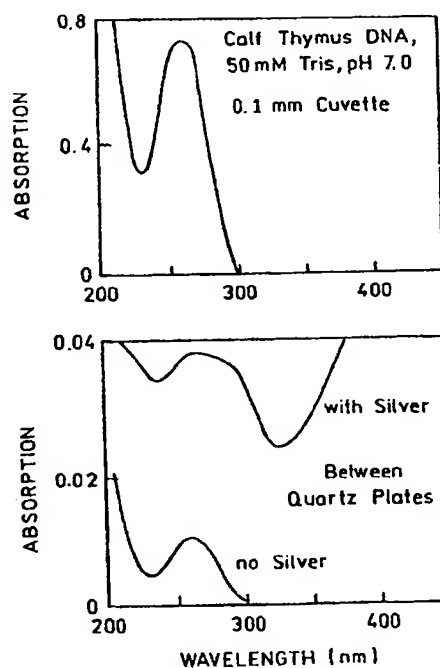


FIG. 2. Top, absorption spectrum of calf thymus DNA. Bottom, absorption spectrum of DNA between two quartz plates, with or without silver island films.

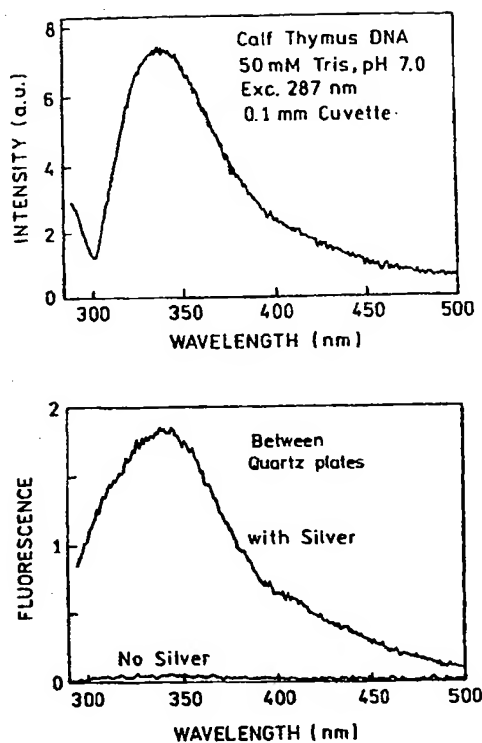


FIG. 3. Top, emission spectra of DNA in the absence of silver islands in a cuvette. Bottom, the same solution between quartz plates (no silver) and between silver island films (with silver).

sum of the DNA and silver island absorption (Fig. 2), which suggests that the islands did not significantly change the extinction coefficient of the DNA.

We examined the emission spectrum of DNA in a thin 0.1 mm cuvette and between the two island films (Fig. 3). Excitation of 287 nm probably resulted in partially selective excitation of the adenine and guanine residues (23–24). Remarkably, the emission is about 80-fold more intense near the metal islands. It is important to notice that this 80-fold increase is a considerable underestimate of the increase displayed by DNA near the particles. The region of enhancement is expected to extend about 200 Å into the solution. Taking into account the two island film surfaces, only about 1/25 of the DNA is near the silver. This suggests that the emission of DNA near the silver is enhanced 2000-fold. This is near the maximum enhancement predicted for a molecule at the optimal distance from an ellipsoid of appropriate size and shape. Since the particle size and geometry is from an ideal, we suspect some of the enhanced emission is due to the amplified field effect described above. This effect can result in a maximum of 140-fold enhancement (14), suggesting a minimum of a 15-fold increase in the quantum yield of the DNA near the island films. It is unlikely that the filed enhancement is maximal. The actual increased quantum yield of DNA is probably greater than 15-fold and less than 2000-fold.

We used time-resolved measurements of the intrinsic DNA intensity decays to evaluate the reason for enhanced emission. One explanation of the increased intensity seen on Fig. 3 could be a decrease in the nonradiative decay rate k_{nr} (Eq. 1), which would result in a longer lifetime (Eq. 1). Another reason for the increased emission could be an amplified incident light field. This effect would result in increased intensity, but the lifetime would be unchanged. Frequency-domain intensity decays are shown in Fig. 4. These measurements were used to reconstruct the more intuitive time-domain decays (Fig. 5). The decays are multiexponential in the absence or presence of metal islands (Table 1). The intensity decays were strongly heterogeneous or multiexponential, which can be seen from the range of decay time from 60 ps to 4.56 ns. The lifetimes of DNA are uncertain because of its weak intrinsic fluorescence. Such a wide range of lifetimes are in agreement with other published reports (25–27). The important conclusion from these experiments is that the mean lifetime ($\bar{\tau}$) of DNA decreased under the same conditions which we observed on 80-fold increase in intensity (Fig. 3). Such a decreased lifetime cannot be explained by a decrease in k_{nr} or increased rate of excitation. However, the decreased lifetime can be explained by an increase in the radiative decay rate.

Let Γ_m represent the rate of the radiative decay due to presence of the metal particles. This new rate changes the quantum in the presence of metal (m) to

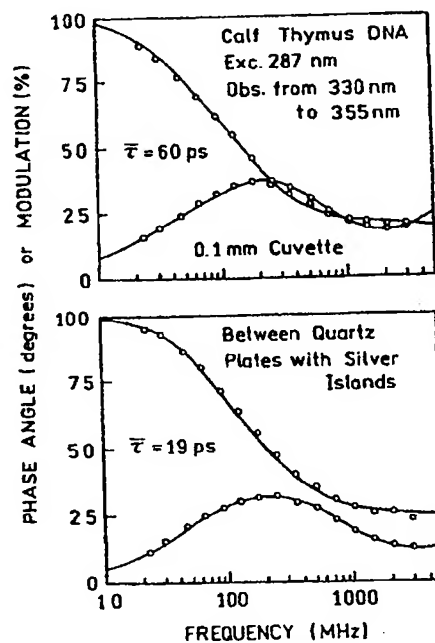


FIG. 4. Frequency-domain intensity decays of calf thymus DNA without metal (top), and between two quartz plates with silver islands film (bottom).

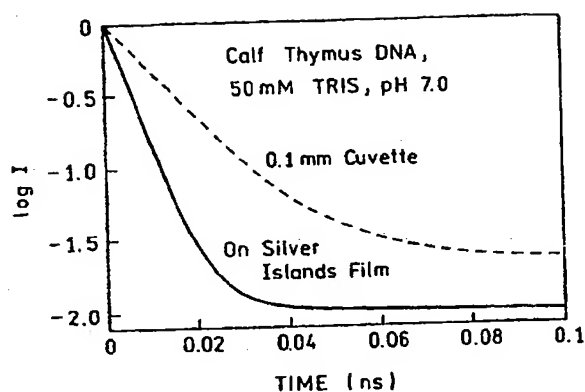


FIG. 5. Time-dependent intensity decays of calf thymus DNA without metal (—) and between silver island films (---).

$$Q_m = \frac{\Gamma + \Gamma_m}{\Gamma + \Gamma_m + k_{nr}} \quad [4]$$

which will be larger than in the presence of the metal. The lifetime in the presence of the metal (τ_m) will be decreased to

$$\tau_m = \frac{1}{\Gamma + \Gamma_m + k_{nr}} \quad [5]$$

Hence an increase in the radiative decay rate of DNA by the metal can explain both the increased intensity and decreased lifetime in the presence of the silver islands. There is no quantitation agreement between the 80-fold increase in intensity and the 3-fold decrease in lifetime. There are numerous possible reasons, including different spatial averaging across the sample by the intensity and lifetime measurements. Nonetheless, the intrinsic DNA lifetime decreased while the intensity increased, demonstrating an increase in the rate of radiative decay.

These effects on fluorescence by metallic particles are reminiscent of surface-enhanced Raman spectroscopy (SERS) (28–29). The absorption of molecules into rough metallic surfaces results in many-fold increases in the Raman signals. The enhanced Raman signals are adequate even for biomedical applications of SERS (30–32). Additionally, it is now thought that the ob-

served enhancements are due to a small subset of the particles which display still stronger enhancements near 10^{15} -fold (33–34). The SERS effect is thought to be due to both the mechanism described above for fluorescence, plus another less understood effect occurring upon molecular contact with the surfaces (15). The case of SERS molecules in contact with the metallic surface are thought to yield the strongest Raman signals. In the case of fluorescence, molecules in direct contact with the metal are thought to be quenched. Hence, the large enhancement found for SERS may not occur surface-enhanced fluorescence, but large effects by a subset of the silver particles can be anticipated due to the high electric fields existing between nearby metallic particles (35). We believe our results with DNA suggest the occurrence of increased radiative rates near metallic surfaces. Such effects are also likely to occur for a wide variety of natural and extrinsic fluorophores. It appears likely that the use of metallic particles or surfaces to enhance fluorescence, will evolve into a field analogous to SERS.

We refer to modification of the radiative decay rates as radiative decay engineering (RDE). The opportunities using RDE are described elsewhere in more detail (36). It is interesting to speculate on the future potential of RDE. Many possibilities can be imagined, such as DNA sequencing using intrinsic base fluorescence, or the use of intrinsic DNA fluorescence with DNA arrays. The need for UV excitation, and the unwanted background with UV excitation, may be eliminated with the use of longer wavelength multi-photon excitation, which is also expected to be enhanced near multiple particles. Another possibility is long range resonance energy transfer (RET). RET is useful for detection proximity between molecules, but only to distances up to about 70 Å. It has been suggested that metallic particles can increase the distance for RET by 10-fold (37–38), allowing detection of proximity of more distant macromolecules.

In closing, the detection of metal-surface enhanced fluorescence from DNA suggests the more widespread use of metallic particles for biochemical and biomedical measurements. Optimization of these effects will require not only spectroscopists, but surface scientists, physicists, and biochemical engineers to create appropriate particles, geometries, and fluorophore distances.

TABLE 1
Fluorescence Intensity Decay Parameters of Calf Thymus DNA in 50 mM Tris, pH 7.0, 20°C

Conditions	$\bar{\tau}$ (ps) ^a	α_1	τ_1 (ps)	α_2	τ_2 (ns)	α_3	τ_3 (ns)	χ^2_R
0.1 mm cuvette	60	0.974	12	0.021	1.17	0.005	4.56	2.7
on silver islands	19	0.989	5	0.007	0.59	0.004	2.38	3.2

^a $\bar{\tau} = \sum_i \alpha_i \tau_i$

^b χ^2_R is the goodness-of-fit parameter calculated with estimated uncertainties in the phase angle and modulation values of 0.3° and 0.007, respectively.

ACKNOWLEDGMENTS

This work was supported by a grant from the NIH, National Center for Research Resource, RR-08119, with partial support from the Juvenile Diabetes Foundation International and the American Diabetes Association.

REFERENCES

1. Benson, S. C., Mathies, R. A., and Glazier, A. N. (1993) *Nucleic Acids Res.* **21**, 5720–5726.
2. Benson, S. C., Zeng, Z., and Glazier, A. N. (1995) *Anal. Biochem.* **231**, 247–255.
3. Smith, L. M., Sanders, J. Z., Kaiser, R. J., Hughes, P., Dodd, C., Connell, C. R., Heiner, C., Kent, S. B. H., and Hood, L. E. (1986) *Nature* **321**, 674–679.
4. Prober, J. M., Trainor, G. L., Dam, R. J., Hobbs, F. W., Robertson, C. W., Zagursky, R. J., Cocuzza, A. J., Jensen, M. A., and Baumeister, K. (1987) *Science* **238**, 336–343.
5. Li, Y., and Glazer, A. N. (1999) *Bioconjugate Chem.* **10**, 241–245.
6. Denijn, M., Schuurman, H.-J., Jacobse, K. C., and De Weger, R. A. (1992) *APMIS* **100**, 669–681.
7. Wiegant, J., Bezrookove, V., Rosenberg, C., Tanke, H. J., Raap, A. K., Zhang, H., Bittner, M., Trent, J. M., and Meltzer, P. (2000) *Genome Res.* **10**, 861–865.
8. Tyagi, S., and Kramer, F. R. (1996) *Nat. Biotechnol.* **14**, 303–308.
9. Tyagi, S., Bratu, D. P., and Kramer, F. R. (1998) *Nat. Biotechnol.* **16**, 49–53.
10. Lipshutz, R. J., Fodor, S. P. A., Gingeras, T. R., and Lockhart, D. J. (1999) *Nat. Genet. Suppl.* **1**, 20–24.
11. Ferea, T. L., and Brown, P. O. (1999) *Curr. Opin. Genet. Dev.* **9**, 715–722.
12. Vigny, P., and Favre, A. (1974) *Photochem. Photobiol.* **20**, 345–349.
13. Morgan, J. P., and Daniels, M. (1980) *Photochem. Photobiol.* **31**, 101–113.
14. Gersten, J., and Nitzan, A. (1981) *J. Chem. Phys.* **75**(3), 1139–1152.
15. Weitz, D. A., Garoff, S., Gersten, J. I., and Nitzan, A. (1983) *J. Chem. Phys.* **78**(9), 5324–5338.
16. Chew, H. (1987) *J. Phys. Chem.* **87**(2), 1355–1360.
17. Kummerlen, J., Leitner, A., Brunner, H., Aussenegg, F. R., and Wokaun, A. (1993) *Mol. Phys.* **80**(5), 1031–1046.
18. Strickler, S. J., and Berg, R. A. (1962) *J. Chem. Phys.* **37**, 814–822.
19. Drexhage, K. H. (1974) *Interaction of Light with Monomolecular Dye Lasers in Progress in Optics* (Wolfe, E., Ed.), pp. 161–232, North Holland Publishing Co., Amsterdam.
20. Barnes, W. L. (1998) *J. Modern Optics* **45**(4), 661–669.
21. Ni, F., and Cotton, T. M. (1986) *Appl. Chem.* **58**, 3159–3163.
22. Laczo, G., Gryczynski, I., Gryczynski, Z., Wicz, W., Malak, H., and Lakowicz, J. R. (1990) *Rev. Sci. Instr.* **61**, 2331–2337.
23. Wilson, R., and Callis, P. (1980) *Photochem. Photobiol.* **31**, 323–327.
24. Georgioliou, S., Braddick, T., Philippetis, A., and Beechem, J. M. (1996) *Biophys. J.* **70**, 1909–1922.
25. Ballini, J. P., Vigny, P., and Daniels, M. (1983) *Biophys. Chem.* **18**, 61–65.
26. Georgioliou, S., Nordlund, T. M., and Saim, A. M. (1985) *Photochem. Photobiol.* **41**(2), 209–212.
27. Plessow, R., Brockhinke, A., Eimer, W., and Kohse-Hoinghaus, K. (2000) *J. Phys. Chem. B* **104**, 3695–3704.
28. Fleischmann, M., Hendra, P. J., and McQuillan, A. J. (1974) *Chem. Phys. Lett.* **26**(2), 163–166.
29. Jeanmaire, D. L., and Van Duyne, R. P. (1977) *J. Electroanal. Chem.* **84**, 1–20.
30. Vo-Dinh, T. (1998) *Trends Anal. Chem.* **17**(8–9), 557–582.
31. Vo-Dinh, T., Stokes, D. L., Griffin, G. D., Volkan, M., Kim, U. J., and Simon, M. I. (1999) *J. Raman Spectr.* **30**, 785–793.
32. Kneipp, K., Kneipp, H., Itzkan, I., Dasari, R. R., and Feld, M. S. (1999) *Curr. Science* **77**(7), 915–924.
33. Nie, S., and Emroy, S. R. (1997) *Science* **275**, 1102–1106.
34. Michaels, A. M., Nirmal, M., and Brus, L. E. (1999) *J. Am. Chem. Soc.* **121**, 9932–9939.
35. Gersten, J. I., and Nitzan, A. (1985) *Surface Science* **158**, 165–189.
36. Lakowicz, J. R. (2001) *Anal. Biochem.* in press.
37. Gersten, J. I., and Nitzan, A. (1984) *Chem. Phys. Lett.* **104**(1), 31–37.
38. Hua, X. M., Gersten, J. I., and Nitzan, A. (1985) *J. Chem. Phys.* **83**, 3650–3659.